The method is of doubtful use for structure determination or quantitative analysis. The wide range of wavelengths, continually varying absorption and profile widths, and other factors create a major difficulty in deriving accurate values of the relative intensities.

Conventional energy-dispersive diffraction methods using white X-rays and a solid-state detector are described in Chapter 2.5 and Section 5.2.7.

2.3.3. Specimen factors, angle, intensity, and profile-shape measurement

The basic experimental procedure in powder diffraction is the measurement of intensity as a function of scattering angle. The profile shapes and 2θ angles are derived from the observed intensities and hence the counting statistical accuracy has an important role. There is a wide range of precision requirements depending on the application and many factors are involved: instrument factors, counting statistics, profile shape, and particle-size statistics of the specimen. *The quality of the specimen preparation is often the most important factor in determining the precision of powder diffraction data.*

D. K. Smith and colleagues (see, for example, Borg & Smith, 1969; see also Yvon, Jeitschko & Parthé, 1977) developed a method for calculating theoretical powder patterns from well determined single-crystal structures and have made available a Fortran program (Smith, Nichols & Zolensky, 1983). This has important uses in powder diffraction studies because it provides reference data with correct I's and d's, free of sample defects, preferred orientation, statistical errors, and other factors. The data can be displayed as recorded patterns by using plot parameters corresponding to the experimental conditions (Subsection 2.3.3.9). Calculated patterns have been used in a large variety of studies such as identification standards, computing intermediate members of an isomorphous series, testing structure models, ordered and disordered structures, and others. Many experiments can be performed with simulated patterns to plan and guide research. The method must be used with some care because it is based on the small single crystal used in the crystal-structure determination and the large powder samples of minerals and ceramics, for example, may have a different composition. Errors in the structure analysis are magnified because the powder intensities are based on the squares of the structure factors.

The Lorentz and polarization factors for diffractometry geometry have been discussed by Ladell (1961) and Pike & Ladell (1961).

Smith & Snyder (1979) have developed a criterion for rating the quality of powder patterns; see also de Wolff (1968*a*).

2.3.3.1. *Specimen factors*

Ideally, the specimen should contain a large number of small equal-sized randomly oriented particles. The surface must be flat and smooth to avoid microabsorption effects, *i.e.* particle interferences which reduce the intensities of the incident and reflected beams and can lead to significant errors (Cline & Snyder, 1983). The specimen should be homogeneous, particularly if it is a mixture or if a standard has been added. Low packing density and specimen-surface displacement (§2.3.1.1.6) may cause significant errors. It is recommended that the powder and the prepared specimen be examined with a low-power binocular optical microscope. Smith & Barrett (1979), Jenkins, Fawcett, Smith, Visser, Morris & Frevel (1986), and Bish & Reynolds (1989) have surveyed methods of specimen preparation and they include bibliographies on special handling problems. Powder diffraction standards for angle and intensity calibration are described in Section 5.2.9.

2.3.3.1.1. *Preferred orientation*

Preferred orientation changes the relative intensities from those obtained with a randomly oriented powder sample. It occurs in materials that have good cleavage or a morphology that is platy, acicular or any special shape in which the particles tend to orient themselves in specimen preparation. The micas and clay minerals are examples of materials that exhibit very strong preferred orientation. When they are prepared as reflection specimens, the basal reflections dominate the pattern. It is common in prepared thin films where preferred orientation occurs frequently or may be purposely induced to enhance certain optical, electrical, or magnetic properties for electronic devices. By comparison of the relative intensities with the random powder pattern, the degree of preferred orientation can be observed.

Powder reflections take place from crystallites oriented in different ways in the instrument geometries as shown in Fig. 2.3.1.2. In reflection specimen geometry with θ–2θ scanning, reflections can occur only from lattice planes parallel to the surface and in the transmission mode they must be normal to the surface. In the Seemann–Bohlin and fixed specimen with 2θ scanning methods, the orientation varies from parallel to about 45° inclination to the surface. The effect of preferred orientation can be seen in diffraction patterns obtained by using the same specimen in the different geometries.

The effect is illustrated in Fig. 2.3.3.1 for *m*-chlorobenzoic acid, $C_7H_5ClO_2$, with reflection and transmission patterns and the pattern calculated from the crystal structure. The degree of preferred orientation is shown by comparing the peak intensities of four reflections in the three patterns:

(*hkl*)	(120)	(200)	(040)	(121)
Reflection	9.8	0.6	1.6	2.5
Transmission	5.2	0.5	0.7	9.3
Calculated	3.0	6.6	4.0	9.1.

Care is required to make certain the differences are not caused by a few fortuitously oriented large particles.

Various methods have been used to minimize preferred orientation in the specimen preparation (Calvert, Sirianni, Gainsford & Hubbard, 1983; Smith & Barrett, 1979; Jenkins *et al.*, 1986; Bish & Reynolds, 1989). These include using small particles, loading the powder from the back or side of the specimen holder, and cutting shallow grooves to roughen the surface. The powder has also been sifted directly on the surface of a microscope slide or single-crystal plate that has been wetted with the binder or petroleum jelly. Another method is to mix the powder with an inert amorphous powder such as Lindemann glass or rice starch, or add gum arabic, which after setting can be reground to obtain irregular particles. Any additive reduces the intensity and the peak-to-background ratio of the pattern. A promising method that requires a considerable amount of powder is to mix it with a binder and to use spray drying to encapsulate the particles into small spheres which are then used to prepare the specimen (Smith, Snyder & Brownell, 1979).

Preferred orientation would not cause a serious problem in routine identification providing the reference standard had a similar preferred orientation and both patterns were obtained with the same diffractometer geometry. However, when accurate values of the relative intensities are required, as in crystal-

structure refinement and quantitative analysis, it may be the major factor limiting the precision.

In practice, it is very difficult to prepare specimens that have a completely random orientation. Even materials that do not have good cleavage or special morphological forms, such as quartz and silicon, show small deviations from a completely random orientation. These show up as errors in the structure refinement and a correction factor is required.

An empirical correction factor determined by the acute angle φ between the preferred-orientation plane and the diffracting plane (hkl)

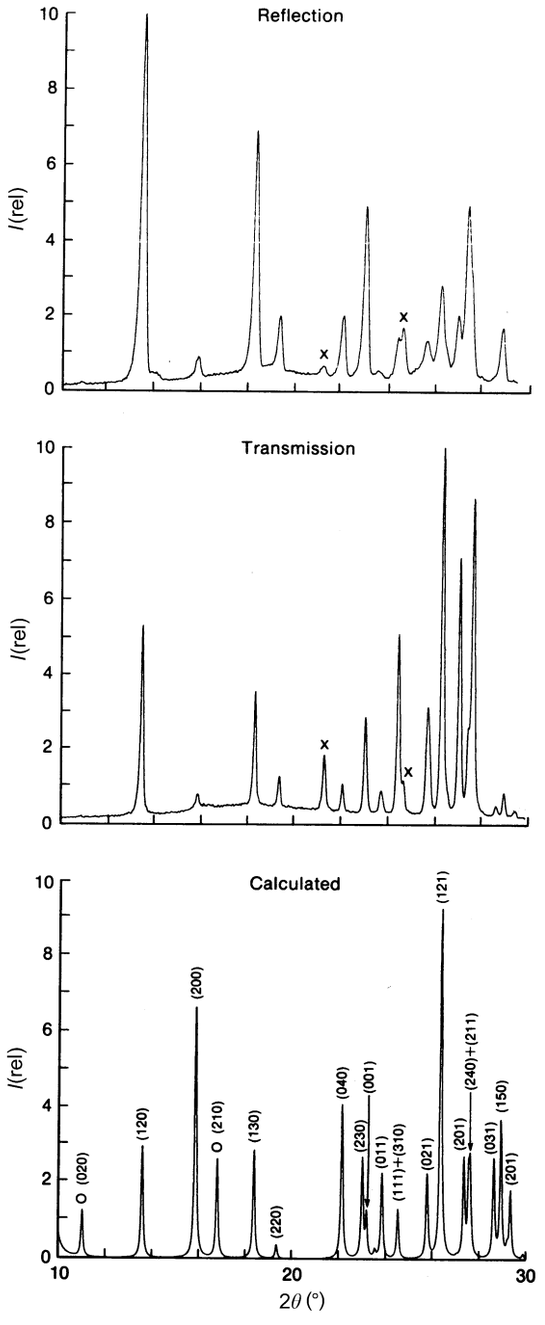

Fig. 2.3.3.1. Differences in relative intensities due to preferred orientation as seen in synchrotron X-ray patterns of *m*-chlorobenzoic acid obtained with a specimen in reflection and transmission compared with calculated pattern. Peaks marked × are impurities, *O* absent in experimental patterns.

Table 2.3.3.1. *Preferred-orientation data for silicon*

$h\ k\ l$	R(Bragg) (%)	GP
1 1 1	1.86	−0.11
2 2 0	2.02	−0.11
3 1 1	2.01	0.17
4 0 0*	0.86	−0.15
3 3 1	1.73	−0.19
4 2 2	2.43	0.04
5 1 1	1.36	0.19
5 3 1	2.44	−0.08
4 4 2	1.69	−0.19
6 2 0	1.25	0.29
5 3 3	2.40	−0.04

* Selected preferred orientation plane.

Table 2.3.3.2. *R(Bragg) values obtained with different preferred-orientation formulae*

	R(Bragg)		
	Si	SiO_2	Mg_2GeO_4
No corrections	3.50	2.57	12.5
Gaussian	1.65	1.60	5.71
Exponential	0.75	1.83	5.30
March/Dollase	0.75	1.64	4.87
Preferred-orientation plane	100	211	100

$$I(\text{corr.}) = I(hkl)P(hkl)\varphi \qquad (2.3.3.1)$$

can be used (Will *et al.*, 1988). Three functions have been used to represent $P(hkl)\varphi$ and the term GP is the variable refined:

$$P(hkl)\varphi = \exp(-\text{GP}\varphi^2) \qquad (2.3.3.2)$$

(Rietveld, 1969) for transmission specimens;

$$P(hkl)\varphi = \exp[\text{GP}(\pi/2 - \varphi^2)] \qquad (2.3.3.3)$$

for reflection specimens; and

$$P(hkl)\varphi = (\text{GP}^2 \cos^2\varphi + \sin^2\varphi/\text{GP})^{-3/2} \qquad (2.3.3.4)$$

(Dollase, 1986).

These functions are quite similar for small amounts of non-randomness. The preferred-orientation plane is selected by trial and error. For example, a modified fast routine of the powder least-squares refinement program with only seven cycles of refinement on each plane for the first dozen allowed Miller indices can be used to find the plane that gives the lowest R(Bragg) value as shown in Table 2.3.3.1. All three functions improve the R(Bragg) value as shown in Table 2.3.3.2 but the evidence is not conclusive as to which is the best. More research is required in this area. Several specimens made of the same material may show different preferred-orientation planes, and in some cases the preferred-orientation plane never occurred in the crystal morphology. A more complicated method examines the polar-axis density distribution using a cubic harmonic expansion to describe the crystallite orientation of a rotating sample (Järvinen, Merisalo, Pesonen & Inkinen, 1970; Ahtee, Nurmela, Suortti & Järvinen, 1989; Järvinen, 1993).

2.3.3.1.2. *Crystallite-size effects*

In addition to profile broadening, which begins to appear when the crystallite sizes are < 1–$2\,\mu m$, the sizes have a strong effect on the absolute and relative intensities (de Wolff, Taylor & Parrish, 1959; Parrish & Huang, 1983). The particle sizes have to be less than about $5\,\mu m$ to achieve 1% reproducible relative intensities from a stationary specimen in conventional diffractometer geometry (Klug & Alexander, 1974). The statistical errors arising from the number of particles irradiated can be greatly reduced by using smaller particles and rotating the specimen around the diffraction vector. This brings many more particles into reflecting orientations.

The particle-size effect is illustrated in Fig. 2.3.3.2 for specimens of NIST silicon standard powder 640 sifted to different size fractions. The powders were packed in a 1 mm deep cavity in a 25.4 mm diameter Al holder using 5% collodion/amyl acetate binder. They were rotated by a synchronous motor (a stepper motor can also be used) around the axis normal to the centre of the specimen surface with the detector arm fixed at the peak position and the intensity recorded with a strip-chart. Rapid rotation, $\sim 60\,r\,min^{-1}$, gives the average peak intensity for all azimuths of the specimen and the small variations result only from the counting statistics. Scaling the intensities to (111) = 100% for the 5–10 μm fraction, the 10–20 μm fraction is 94%, 20–30 μm 88% and > 30 μm 59%. The decrease is probably due to lower particle-packing density and increasing interparticle microabsorption. The > 5 μm fraction = 95% may be due to the larger ratio of oxide coating around the particles to the mass of the particles.

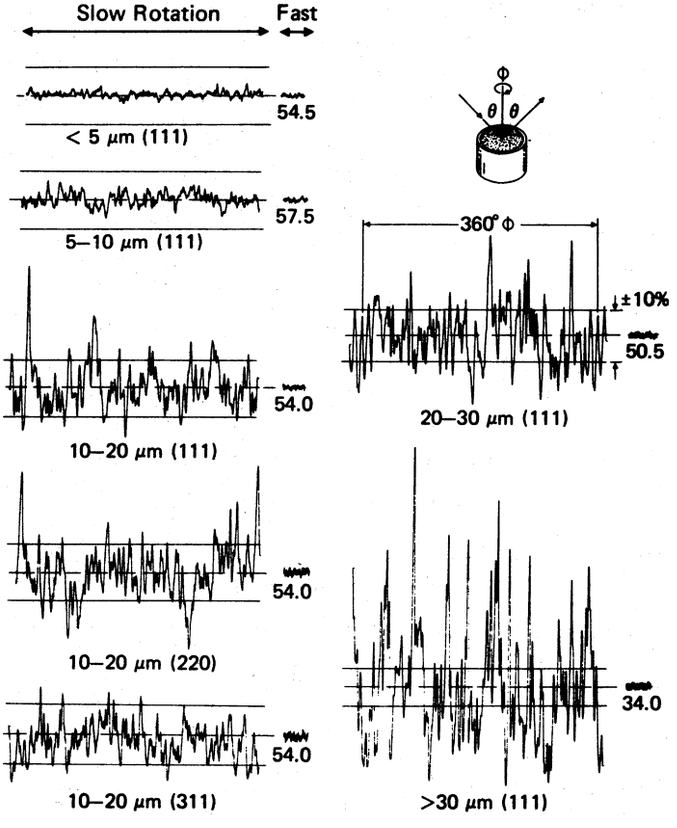

Fig. 2.3.3.2. Effect of specimen rotation and particle size on Si powder intensity using a conventional diffractometer (Fig. 2.3.1.3) and Cu $K\alpha$. Numbers below fast rotation are the average intensities.

Slow rotation, $\sim 1/7\,r\,min^{-1}$, shows the variation of the peak intensity with azimuth angle φ. The pattern repeats after 360° rotation and the magnitude of the fluctations increases with increasing particle sizes and resolution. There is no correlation between the fluctations of different reflections, as can be seen by comparing the 111, 220 and 311 reflections of the 10–20 μm specimen (lower left side) for which the incident-beam intensity was adjusted to give the same average amplitude. The horizontal lines are ±10% of the average. This shows the magnitude of errors that could occur using stationary specimens. Similar particle-size effects were found using the integrated intensities derived from profile fitting. The above discussion and Fig. 2.3.3.2 refer to a continuous scan. If the step-scan mode is used to collect data, it is clearly not necessary to rotate the specimen through more than one revolution at each step.

The rotating specimen also averages the in-plane preferred orientation but has virtually no effect on the planes oriented parallel to the specimen surface. The slow rotation method is useful in testing the grinding and sifting stages in specimen preparation. When calibrated with known size fractions, it can be used as a rough qualitative measure of the particle sizes.

2.3.3.2. *Problems arising from the Kα doublet*

A common source of error arises from the $K\alpha$ doublet which produces a pair of peaks for each reflection. The separation of the Cu $K\alpha_1$, $K\alpha_2$ peaks increases from 0.05° at 20°2θ to 1.08° at 150°2θ. The overlapping is also dependent on the instrument resolution and may cause errors in the peak angles and intensities when strip-chart recording or peak-search methods (described below) are used. The $K\alpha_1$ wavelength is generally used to calculate all the d's even when the low-angle peaks are unresolved. In the region where the doublet is only slightly resolved, the apparent $K\alpha_1$ peak angle is shifted to higher angles because of the overlapping $K\alpha_2$ tail and similarly the peak intensities will be in error. The relative peak intensities of a reflection with superposed doublet compared to a resolved doublet could have an error as large as 50%. Relative peak intensities are used in the ICDD standards file and cause no problem because the unknowns are measured in the same way. The integrated intensity avoids this difficulty but is impractical to use in routine identification.

Rachinger (1948) described a simple graphical procedure for removing $K\alpha_2$ peaks. The method causes errors because it makes the incorrect assumption that $K\alpha_2$ is the exact half-scale version of $K\alpha_1$. Ladell, Zagofsky & Pearlman (1975) developed an exact algorithm using the actual mathematical shapes observed with

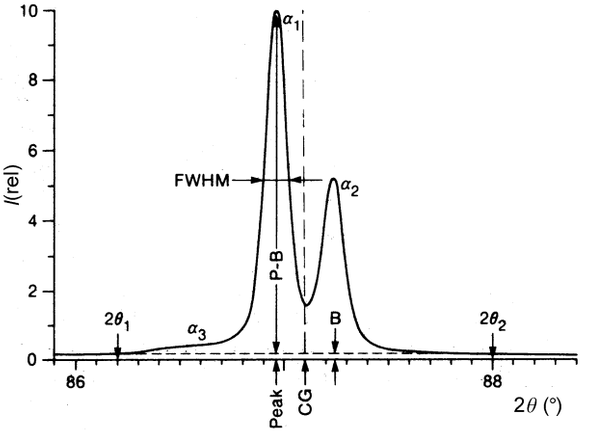

Fig. 2.3.3.3. Various measures of profile.

references